IEEE Access
Multidisciplinary ⁝ Rapid Review ⁝ Open Access Journal

Received July 19, 2021, accepted July 27, 2021, date of publication August 3, 2021, date of current version August 13, 2021.

Digital Object Identifier 10.1109/ACCESS.2021.3102308

A Robust Timing and Phase Offset Estimation Technique for CPM-DSSS-Based Secured Communication Link

SAIMA SHEHZADI [1], SHAHZAD AMIN SHEIKH [1], FARZANA KULSOOM [2], MUHAMMAD ZEESHAN [1], AND QASIM UMAR KHAN [1]

[1]Department of Electrical Engineering, College of Electrical and Mechanical Engineering, National University of Science and Technology, Islamabad 44000, Pakistan

[2]Department of Telecommunication Engineering, University of Engineering and Technology, Taxila 47050, Pakistan

Corresponding author: Saima Shehzadi (saima.shahzadi@ceme.nust.edu.pk)

ABSTRACT Continuous Phase Modulation–Direct Sequence Spread Spectrum (CPM-DSSS) is a promising scheme for a secured Point-to-Point (P2P) communication system having Anti-Jamming (AJ) capabilities. However, like other communication systems, synchronization of CPM-DSSS based systems is required for reliable detection of data. This paper presents a novel algorithm for estimating the timing and phase offset for binary full-response CPM-DSSS based systems. A burst mode transmission is considered here, and within each burst, a training sequence is embedded along with data. Firstly, the entire burst is spread using DSSS and then modulated with CPM, which is later upconverted and passed on to the channel. After down-conversion at the receiver, the proposed algorithm estimates timing and phase offset from the received spread training sequence. Then estimation accuracy of the proposed algorithm is compared with the state-of-the-art. The results indicate that the proposed joint estimator is superior by 9 dB and 10 dB for the estimation of timing and phase offset, respectively, as compared to the existing algorithm. Furthermore, the estimator's variance for three different frequency pulses is compared with Modified Cramer-Rao Bound (MCRB). The results suggest that the phase offset estimator's variance approaches MCRB for all Signal-to-Noise Ratios (SNRs). The effectiveness of the proposed algorithm in the multipath fading channel is also demonstrated.

INDEX TERMS Timing offset, carrier phase offset (CPO), continuous phase modulation-direct sequence spread spectrum (CPM-DSSS) scheme, point-to-point (P2P) communication.

I. INTRODUCTION

In Point-to-Point (P2P) communication, machines and equipment communicate with each other directly, without or with very little involvement of any network infrastructures. It is usually based on short-range communication and demands low latency and high throughput. With the technological advancements, 5G promises to offer connection anywhere, anytime within cellular network: smart objects in smart cities, vehicles, and machines. For example, in 5G its potential applications are Machine-to-Machine (M2M), Device-to-Device (D2D), Vehicle-to-Vehicle (V2V) communication. The application areas span from controlling autonomous vehicles, traffic lights, smart healthcare devices, smart home appliances, military vehicles, and to all type of machine communication which require low latency and high throughput. In P2P links, the devices frequently enter and leave the network; therefore, the security requirement of such transmission links is of paramount importance as they are more prone to security risks, including eavesdropping, jamming and denial of service attack. Each of these risks impact the performance and reliability of the communication link. For example, in eavesdropping, an intruder can listen to the exchange of information in a communication link, which could be severe security threat depending on the information and motives of the intruder [1]. The Anti-Jamming (AJ) induces an ability in the communication link to prevent itself from being blocked by tuning into the transmitter's frequency [2], [3].

The above-mentioned security threats have been dealt in the literature by employing encryption, Frequency Hopping Spread Spectrum (FHSS), or Direct Sequence Spread

The associate editor coordinating the review of this manuscript and approving it for publication was Yiming Huo.

Spectrum (DSSS). Although the encryption techniques are considerably effective in acquiring security, they require a lot of processing and power consumption. In contrast to that, most of the devices in P2P communication are assumed to be battery-held and low-powered. The FHSS divides the available spectrum into separate bands and hops the frequencies among these bands. On the other hand, DSSS encodes each data bit into chips and spreads it over the entire bandwidth. At high data rates FHSS is an expensive option for which DSSS provides a viable solution [4]. Although FHSS and DSSS provide AJ, however, both are incapable of utilizing the spectrum efficiently. Orthogonal Frequency Division Multiplexing Access (OFDM) is a well-known technique to enhance spectral efficiency and system throughput [5]. OFDM is very successful in utilizing the spectrum efficiently; however, it is prone to security concerns, sensitive to frequency and timing offsets. Therefore, FHSS is employed in literature along with OFDM to provide spectral efficiency and anti-jamming capabilities. Another useful feature of FHSS-OFDM based system is for battery held devices since they provide better power efficiency.

Besides all the benefits of FHSS, it suffers several problems, including the overhead of frequency hopping, synchronization, and reconnections. The FHSS-OFDM based scheme is also sensitive to disguised jamming scenarios [6]. The alternative choice DSSS does not have frequency and synchronization overheads; therefore, it is much faster as compared to FHSS based systems. It also has higher throughput due to better processing efficiency. Nevertheless, the DSSS suffers inefficient spectral utilization and high power consumption. A combination of Continuous Phase Modulation (CPM) and DSSS can be employed to overcome these drawbacks [7]. A CPM-DSSS offers several valuable features: firstly, the constant envelope of CPM enables the utilization of nonlinear amplifiers, which are more economical and power-efficient [8]. Secondly, the spread spectrum signal yields a low probability of intercept, anti-jamming, anti-interference, and high-frequency efficiency [9]. Finally, in terms of the band-limited case, the narrow Power Spectral Density (PSD) of CPM will enhance the processing gain [10]. The increased processing gain provides interference tolerance to the CPM-DSSS scheme.

However, the synchronization of CPM-DSSS system is complex due to inherent memory of CPM Modulation. Non-ideal conditions of the channel and noise affect the clock and phase between transmitter and receiver in communication systems. The knowledge of synchronization parameters such as carrier phase and timing offset are vital for the reliable detection of signals [11], [12]. If the received signal is not synchronized accurately it can degrade the received signal by amplitude reduction or phase rotation.

In this paper, a robust Data Aided (DA) algorithm is proposed for the estimation of timing and phase offset of CPM-DSSS scheme, applicable to next-generation P2P communication systems as well as military Software Defined Radios (SDRs) for example, the proposed CPM-DSSS scheme combines the benefits of CPM and DSSS schemes, i.e., higher spectral efficiency and strong anti-jamming capability [13], to make it a strong candidate for tactical wideband SDR waveforms and other secure and high throughput networks. Also the proposed algorithm can be used to estimate the constant sampling clock offsets (SCOs) in such systems. The SCO is mainly produced by the difference in the frequency of the transmitter sampling clock of digital-to-analog converter and the receiver's sampling clock of analog-to-digital converter [14].

Data aided and non-data aided schemes have been commonly used in the literature. In this work, a data-aided approach has been utilized to estimate our desired parameters. Although a non-data-aided approach seems attractive from a security perspective because it avoids sending the known data [15]. Alternately, the data-aided method is better in terms of Bit-Error-Rate (BER) performance than the non-data-aided approach [15]. Therefore, data aided approach has been considered and the security aspect is incorporated with the employment of DSSS. Our main contributions are listed as follows:

- A novel DA algorithm is proposed for the joint estimation of timing offset and carrier phase offset for the CPM-DSSS scheme.
- A novel usage of above algorithm for finding the constant sampling clock offset in physical layer of CPM-DSSS based SDR waveforms is proposed.
- The effectiveness of the proposed algorithms for CPM-DSSS is verified through simulations in multipath channel.

A. RELATED WORK

Some research work related to estimate symbol timing and phase for the CPM system is already done in the literature. For example, Morelli and Vitetta [16] presented novel Non-DA algorithms for MSK-type modulations which jointly estimates timing and carrier phase. MSK-type modulation is subclass of CPM with alphabet size equal to 2 and modulation index of 0.5 [17]. This algorithm is based on Maximum Likelihood (ML) method and it is suitable for digital implementation as it has a feed forward structure. Huber and Liu [18] proposed a DA ML joint timing and phase synchronization algorithm. This algorithm uses non-orthogonal exponential basis functions for the transformation of the CPM signal. Then, Tang and Shwedyk [19] estimate the symbol timing and carrier phase for CPM modulation by signal space decomposition of the CPM signal in the Walsh signal space. In another work, Zhao and Stuber [20] proposed a DA algorithm for joint phase and timing estimation. This algorithm is based on the Minimum Mean-Square Error (MMSE) criteria and it is robust in time-variant channels. However, its Mean Square Error (MSE) performance is shown to be much larger than the Cramer-Rao Bound (CRB) even at higher Signal-to-Noise Ratios (SNRs). Hosseini and E. Perrins in [21], [22] presents DA ML, a feed-forward algorithm for burst mode CPM system over Additive White Gaussian Noise (AWGN).

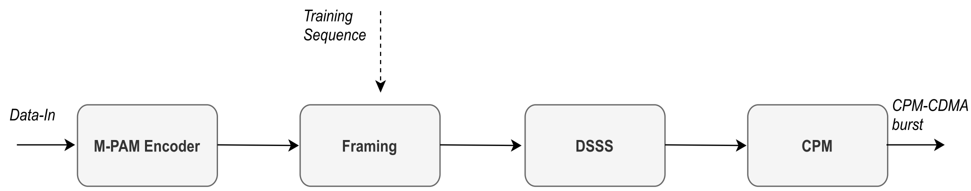

FIGURE 1. CPM-DSSS burst formation.

This algorithm estimates the symbol timing, frequency offset, and carrier phase jointly. The estimator's MSE performance is quite close to the CRB for all above mentioned parameters at SNRs as low as 0 dB. The [23] presents the three synchronization techniques which have employed statistical aspects of the full-response CPM signals considering modulation index h equal 1. The algorithms presented in this paper are non-DA, have feed-forward structure, suitable for burst-mode transmissions, and are used to estimate the symbol timing, carrier frequency offset and carrier phase. These three schemes are: the sample-point scheme, the mean-function scheme, and the correlation function (CF) scheme. Among three schemes the CF scheme is most effective in terms of computation complexity. The algorithms are claimed to work for M-ary CPM signal but the simulation results are presented for binary CPM signals with Rectangular (REC) and Raised-Cosine (RC) frequency pulses. The MSE performance of all the synchronization parameters as a function of SNR is compared with the modified-CRB (MCRB) and it is concluded that the performances of only the frequency offset estimator and timing offset estimator are close to the theoretical limits at high SNR. Similarly, in [24] authors discussed the joint frequency and timing recovery schemes for full-response CPM signals with modulation index of 1 by investigating the property of the two different types of the auto correlation functions for CPM scheme. Although all the algorithms mentioned above are designed for the CPM system, they do not have any anti-jamming capability, which effectively means a system with compromised security. A CPM-DSSS based work [25] presents an interference-insensitive synchronization schemes by employing Pseudo-Noise (PN) preamble of arbitrary length for Transmit Only (TO) Wireless Sensor Networks (WSNs). In that research work, frame synchronization, fractional timing offset, and carrier synchronization have been performed separately. On the other hand, we have jointly estimated the synchronization parameters with the ML algorithm in our work. In essence, their system and algorithm to determine synchronization parameters are entirely different than the work given in this paper. Thus in the light of the above discussion, we conclude that the joint timing and carrier phase offset estimation with a burst mode for CPM-DSSS based P2P systems is an open research problem to the best of the author's knowledge.

The rest of the paper is organized as follows: Section II presents the system model, Section III illustrates the proposed estimation algorithm, Section IV gives the results and discussion part, and finally, Section V concludes the paper.

II. THE SYSTEM MODEL

In this work, a burst mode transmission model is considered for P2P communication. Each burst comprises of training sequence and data. The formation of CPM-DSSS burst is depicted in Fig. 1. It can be seen that the binary data stream is first passed through a 2-PAM encoding block where 2 is the alphabet size and its values are from the set $\{-1, 1\}$. Then a known training sequence is added to the encoded bit stream in the framing block to form a burst. At this stage, the length of the training sequence consists of L_0 symbols, each with the duration T_s such that the size of the whole training sequence is $T_0 = L_0\, T_s$. The training sequence used for burst formation is similar to burst mode CPM as given in [21], [22]. Each symbol in the training sequence is also in 2-PAM form. Then, each symbol in the burst is mapped to chips called d_i using the direct sequence spreading by employing Golay complementary sequence [26], [27] of the length $L_c = 8$ so that each bit per symbol interval T_s can be transmitted. After spreading of whole burst, the length of spread training sequence is represented as $T_0' = L_0\, L_c T_c = WT_c$. Where, T_c is chip interval and $W = L_0\, L_c$. Finally, the chips d_i are transformed to CPM phase function as presented in [28]. This phase function for the spread form of the training sequence is given in (1),

$$\varphi(t, \mathbf{d}) = 2\pi h \sum_{i=1}^{L_c L_0 - 1} d_i q(t - iT_c) \tag{1}$$

where, $\mathbf{d} \triangleq (d_1, d_2, \ldots, d_{L_0\, L_c - 1})$ is a vector and d_i is specific element of the vector. The $q(t)$ in (1) is a phase smoothing response function with the restriction that $q(t) = 0,\ t < 0$ and $q(t) = 1/2$ for $t > LT_c$. This function describes how the underlying phase evolves with time. Basically, $q(t)$ is integral of frequency pulse $g(t)$ utilized i.e., $q(t) = \int_0^t g(\tau)d\tau$ with the duration LT_c [29], [30]. It is important to mention that when $L = 1$ the CPM signal is full-response signal and if $L > 1$ it is called partial response signal. In (1) h is the modulation index. In this work, we have assumed only binary full-response case with the value of modulation index 0.5. The three types of frequency pulses $g(t)$ which are considered in this work are Gaussian pulse with time bandwidth product (BT_c) of 0.3, REC pulse, and RC pulse.

Now the baseband representation of CPM modulated spread training sequence is given in (2)

$$s(t, \mathbf{d}) = e^{j\varphi(t,\mathbf{d})} \tag{2}$$

Let r(t) represents the complex baseband received signal in AWGN and can be put down as in [31].

$$r(t) = s(t, \mathbf{d}, \theta, \tau) + w(t) \tag{3}$$

$$r(t) = \sqrt{\frac{E_c}{T_c}} e^{j\theta} e^{j\varphi(t-\tau,\mathbf{d})} + w(t) \tag{4}$$

where, E_c is the energy per transmitted chip, θ is the difference between the phase of the transmitting carrier and the receiver's oscillator, τ is the timing difference between the transmitter and receiver. Then, $w(t)$ is complex baseband AWGN with zero mean and N_0 PSD. The unknown timing offset is limited to the interval $0 \leq \tilde{\tau} < T_c$ and the unknown carrier phase is limited to the interval $(0, 2\pi)$. The information carrying phase $\varphi(t, \mathbf{d})$ in the n_{th} chip duration $[nT_c, (n+1)T_c]$, which will be denoted as $\varphi(t, \mathbf{d_n})$ and defined as

$$\varphi(t, \mathbf{d}_n) = 2\pi h \sum_{i=-\infty}^{n} d_i q(t - iT_c) \tag{5}$$

where, $\mathbf{d}_n \triangleq (\ldots, d_{n-1}, d_n)$ is vector that is containing all the chip values starting from $-\infty$ up till the current time i.e., n. These chips are selected from M-ary information-carrying chips selected from the alphabet $\pm 1, \pm 3, \cdots, \pm(M-1)$. Where M is the alphabet size, in our case M = 2.

III. THE PROPOSED ESTIMATION ALGORITHM

The log likelihood function [31] for the unknown parameters θ and τ for the time span of training sequence is given as in (6),

$$\begin{aligned} \Lambda(\tilde{\tau}, \tilde{\theta}) &= Re\left\{ e^{-j\tilde{\theta}} \int_{\tilde{\tau}}^{WT_c+\tilde{\tau}} r(t) e^{-j\varphi(t-\tilde{\tau},\mathbf{d})} dt \right\} \\ &= Re\left\{ e^{-j\tilde{\theta}} Z(\mathbf{d}, \tilde{\tau}) \right\} \end{aligned} \tag{6}$$

where $\tilde{\tau}$, $\tilde{\theta}$ are the trial values for the timing offset, carrier phase offset respectively, also

$$Z(\mathbf{d}, \tilde{\tau}) \cong \int_{\tilde{\tau}}^{WT_c+\tilde{\tau}} r(t) e^{-j\varphi(t-\tilde{\tau},\mathbf{d}) dt} \tag{7}$$

and W is number of chips used on which estimation is based. As mentioned earlier, we have used $W = L_c L_0$. It is assumed that the spread training sequence $\mathbf{d}$ is known at the receiver and that θ and τ can be considered constant over the period of observation interval WT_c. Since the CPM-DSSS scheme is wide band in nature resulting in high throughput [13] therefore the bit duration (T_b) and consequently the chip duration (T_c) is very small i.e., in order of μ sec. Because of this small observation interval, we have assumed that the timing and phase offsets are constant throughout the observation interval WT_c. From the above equation the ML estimates [31] of θ is simply

$$\hat{\theta} \triangleq \arg\{Z(\mathbf{d}, \hat{\tau})\} \tag{8}$$

provided that $Z(\mathbf{d}, \hat{\tau})$ is known. Where $\hat{\tau}$ is the value that maximizes $|Z(\mathbf{d}, \tilde{\tau})|$ in the joint estimation i.e.

$$\hat{\tau} = \arg \max_{\tilde{\tau}} |Z(\mathbf{d}, \tilde{\tau})| \tag{9}$$

In general, it is difficult to obtain $Z(\mathbf{d}, \tilde{\tau})$ for CPM modulation, but we can obtain its approximate form by approaching the phase response of RC and Gaussian pulse to the REC frequency pulse phase response as done in [21], [22]. Let's re-write the approximate form of (7) i.e. $Z(\mathbf{d}, \tilde{\tau})$ for the duration of training sequence as

$$Z(\mathbf{d}, \tilde{\tau}) \approx \sum_{n=0}^{W-1} \int_{nT_c}^{(n+1)T_c} r(t) e^{-j\varphi(t-\tilde{\tau},\mathbf{d_n})} dt \tag{10}$$

The rectangular frequency pulse phase response during the chip interval is given as in [32]

$$\varphi(t, \mathbf{d_n}) = \phi_n + \pi h d_n \frac{t - nT_c}{T_c} \quad nT_c \leq t \leq (n+1)T_c \tag{11}$$

where, ϕ_n is the initial phase at the current chip interval. Thus we have,

$$\varphi(t - \tilde{\tau}, \mathbf{d_n}) = \phi_n + \pi h d_n \frac{(t - nT_c - \tilde{\tau})}{T_c} \tag{12}$$

Putting (12) in (10)[1]

$$Z(\mathbf{d}, \tilde{\tau}) \approx \sum_{n=0}^{W-1} \int_{nT_c}^{(n+1)T_c} r(t) s^*(t) e^{j\left(\pi h d_n \frac{\tilde{\tau}}{T_c}\right)} dt \tag{13}$$

The computation of (9) requires different trial values of $\tilde{\tau}$ and its values lie in the interval $[0, T_c)$. Once the $\hat{\tau}$ is estimated using (9) and (13) then the phase estimates are found using (8). It is worth mentioning that our proposed estimation algorithm and the algorithm presented in [21], [22] are both ML algorithms but the main difference between the two algorithms is that in case of [21], [22] the training sequence is approximated with 1-REC frequency pulse phase response at symbol level. While in our case, the training sequence is initially spread using DSSS followed by the approximation of the phase response of the training sequence with 1-REC pulse phase response at the chip level.

The overall system description for the joint estimation of timing and phase offset is outlined in the Framework, and its block diagram is drawn in Fig. 2 where the discrete time version of (13) is used in which the integrals are replaced with the summation. We also assume that the $r(t)$ in above equation is sampled N times per chip interval i.e., $r[k] = r(kT_c/N)$. Based on the block diagram drawn in Fig. 2, the computational complexity can be calculated in terms of a number of multiplications and number of additions as in [33]. Our joint phase and timing offset estimator requires 3 NW complex multiplications and 2 NW complex addition, where $W = L_o L_c$. In [22], which is an extended version of [21] computational complexity has been calculated in terms of number of operations. The algorithm presented in [21] and [22] are computationally more extensive as it aims to jointly estimate

[1] Please see appendix for derivation

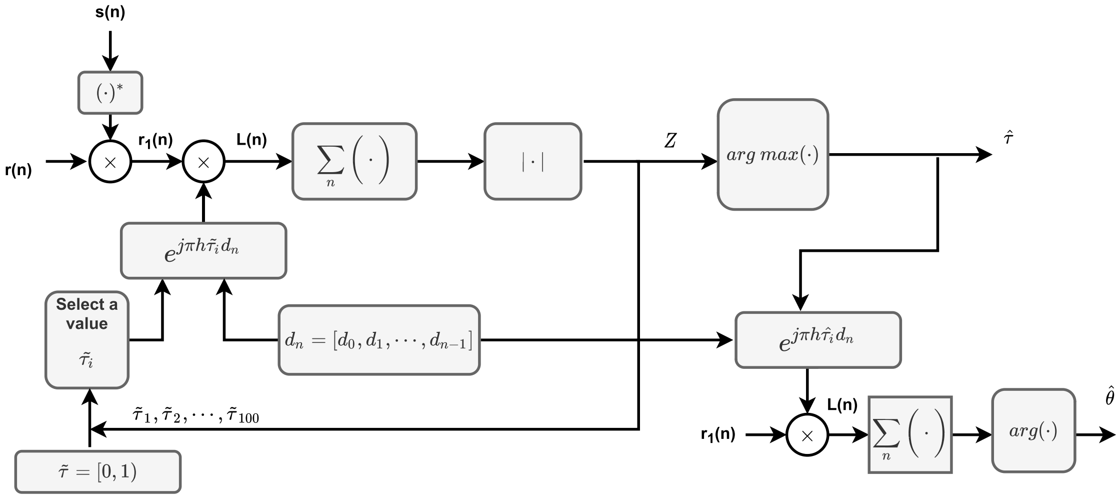

FIGURE 2. Block diagram of the proposed timing and phase offset estimator.

Framework : Joint Estimation of Timing and Phase Offset

Step-1: CPM-DSSS burst is formed at transmitter side as shown in Fig. 1.

Step-2: After passing through channel, $\mathbf{r(t)}$ is the received signal.

Step-3:(Timing Offset) Next, the known CPM-DSSS training sequence at the receiver $s^*(t)$ is multiplied by the received training sequence $r(t)$ for full length of the received training sequence. Now the first the timing offset τ is estimated in two steps

(a) Given $\mathbf{d}$, the function $|Z(\mathbf{d}, \tilde{\tau})|$ is evaluated for different trials value of τ i.e. $\tilde{\tau}$ using (13).

(b) Next the estimates of timing offsets $\hat{\tau}$ is found using (9) i.e., the value of $\tilde{\tau}$ that maximizes the absolute value of the (13) is chosen as timing offset estimates.

Step-4:(Phase Offset) The phase offset estimates are evaluated as follows

(a) Given $\mathbf{d}$, the function $Z(\mathbf{d}, \hat{\tau})$ is evaluated for estimated value τ i.e. $\hat{\tau}$ using (13).

(b) Next the estimates of phase offsets $\hat{\theta}$ is found using (8).

Step-5: The estimated values are used to compensates the timing and phase offset.

Step-6: After the compensation the reverse operations of Fig. 1 are performed to get the original bit stream.

three parameters with a highly optimized training sequence specific to the algorithm. On the other hand, our proposed algorithm uses a more generic training sequence for the joint estimation of the timing offset and carrier phase, without using a highly complicated FFT operation. In [22] the joint estimation algorithm requires $2NL_o + 3$ complex multiplications and $NL_o + 1$ addition. In addition to that their system requires NL_o real multiplications and $K_f NL_o$ additions where the complexity due to FFT operation is not included.

IV. RESULTS AND DISCUSSION

This section elaborates simulation results for the proposed estimation algorithm. The parameters used for the simulation are as follows: for spreading, Golay code has been used [26], [27] and the spreading sequence length is taken as $L_c = 8$. The training sequence used in this work is similar as in [21], [22] for CPM burst with the length of training sequence given as $L_0 = 64$ symbols. The spread training sequence is modulated with full-response CPM having binary alphabet and modulation index 0.5. The performance metric used is the estimators' variance [34] and it is given in (14),

$$var(\hat{\epsilon}) = \frac{1}{M}\sum_{i=1}^{M}(\hat{\epsilon}_i - \hat{E}(\hat{\epsilon})) \tag{14}$$

where, $\hat{E}$ is the sample mean of the estimate $\hat{\epsilon}$ and is given in (15).

$$\hat{E}(\hat{\epsilon}) = \frac{1}{M}\sum_{i=1}^{M}\hat{\epsilon}_i \tag{15}$$

where, M is the number of realizations. For instance, in this work $M = 2000$ is considered.

A. PERFORMANCE OF PROPOSED TIMING OFFSET ESTIMATOR

This subsection presents the performance comparison of the proposed timing offset estimator with other works in literature i.e. [21], [22], [34]. Furthermore, the proposed timing offset estimator's performance is presented for various frequency pulses such as Gaussian, REC, and RC. The estimator's variance versus SNR are compared with the respective MCRB. Finally, to investigate the robustness of the proposed timing offset estimator in multipath channel, Stanford University Interim (SUI)-3 channel is employed and comparison of its performance is done with AWGN channel. Fig. 3

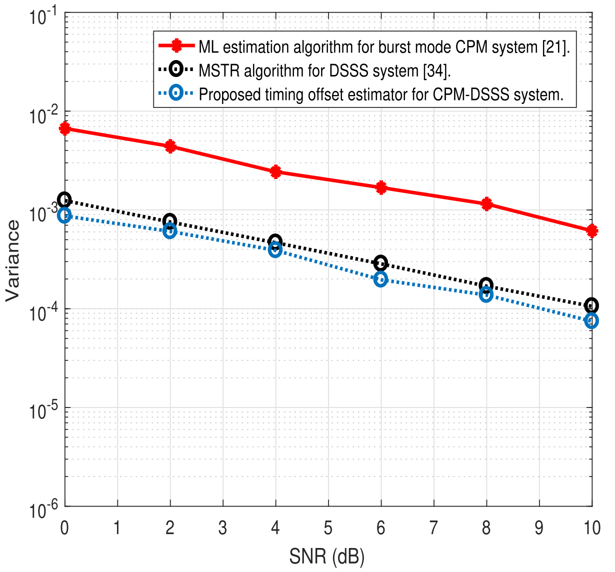

FIGURE 3. Comparison of the variance of timing offset estimator for the proposed algorithm of CPM-DSSS system versus SNR and ML algorithm of CPM system [21] and MSTR algorithm for DSSS system [34] when the timing offset value to be estimated is chosen randomly from $[0, T_c)$ at each SNR.

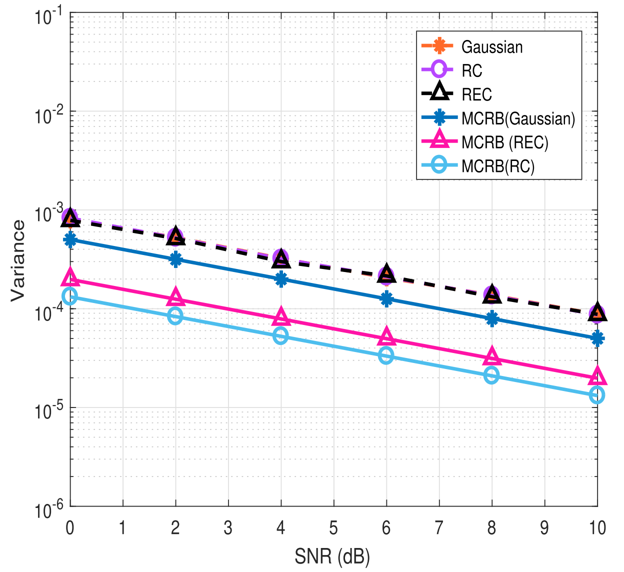

FIGURE 4. Comparison of variance of timing offset estimator for different CPM-DSSS system versus SNR with MCRB for different frequency pulse shapes.

shows the comparison of variances versus SNR of the proposed timing offset estimator for the CPM-DSSS system, ML estimator for burst mode CPM system [21], [22] and Modified Square Timing Reovery (MSTR) Algorithm for standard DSSS system [34]. The value of timing offset is randomly chosen for each SNR from range $[0, T_c)$. It can be noticed that when the SNR increases, the mean square error starts decreasing, which indicates the improvement in timing offset estimation. For example, at SNR $= 1$ dB the variance of proposed timing offset estimator for CPM-DSSS system is 0.59×10^{-3} dB whereas variance of ML estimator for CPM system [21], [22] is 4.9×10^{-3} dB. Because the variance of the proposed algorithm for CPM-DSSS system is smaller than the ML algorithm for the CPM system [21], [22]. Therefore, it can be inferred that the proposed algorithm for the CPM-DSSS system is outperforming its counterpart. Next, we compare the proposed algorithm performance with the Modified Square Timing Recovery (MSTR) algorithm given in [34]. As can be seen in the Fig. 3, the estimation performance of the proposed algorithm is approximately 0.1 dB better than MSTR algorithm for BPSK-DSSS systems at all SNRs.

Later, Fig. 4 shows the comparison of variance of timing offset estimates versus SNR with MCRB for different frequency pulses [35]. The fractional delay or timing offset and phase offset are considered to be $0.25T_c$ and $\frac{\pi}{2}$ radians in this case. The proposed timing offset estimator for Gaussian frequency pulse is showing 2 dB degradation in performance than MCRB. On the other hand, when the REC frequency pulse is used, it is showing 8 dB poor performance as compared to MCRB. However, when RC frequency pulse is used [35] this degradation in performance is 2 dB worst when the REC pulse is used.

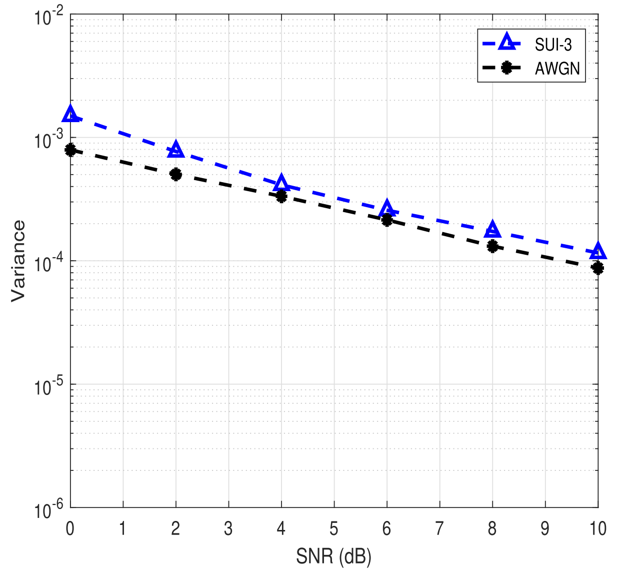

FIGURE 5. Performance of the timing offset estimator in terms of variance of timing offset estimator versus SNR for AWGN and multipath SUI-3 channel.

Finally, Fig. 5 shows the performance comparison of the proposed timing offset estimator for both AWGN and multipath SUI-3 fading channel model. The SUI-3 channel represents a terrain with moderate to high tree density and weak Line-of-Sight (LOS) [36]. The specifications of the SUI-3 channel model are given in Table 1. The K-factor in this table represents the ratio of LOS components to Non-LOS (NLOS) components. For LOS, the K-factor is non-zero. It can be seen in Fig. 5 that the multipath SUI-3 channel performance degradation is almost 2 dB at low SNRs as compared to AWGN channel, whereas it reduces to 1 dB at high SNRs. Thus we conclude that our proposed timing offset estimator is robust in multipath fading channel as well.

TABLE 1. SUI-3 channel model specification.

	Tap 1	Tap 2	Tap 3
Delay (μs)	0.0	0.4	0.9
Power (dB)	0	-5	-10
K-factor	1	0	0
Doppler (Hz)	0.4	0.3	0.5

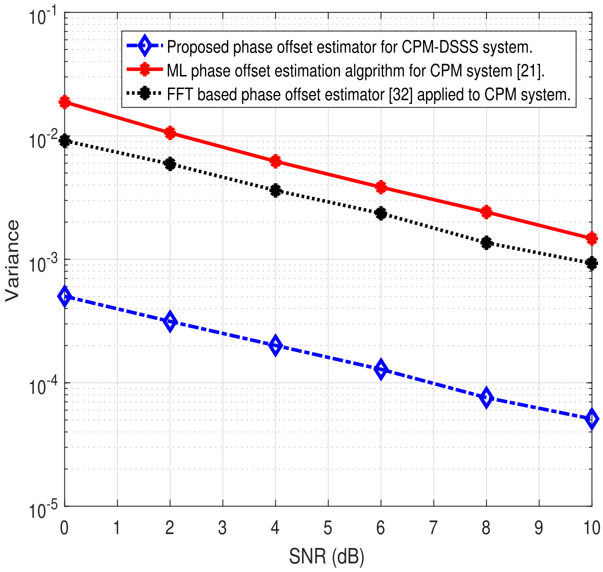

FIGURE 6. Comparison of variance of carrier phase offset estimates versus SNR for proposed estimator for CPM-DSSS system with other works in literature. The phase offset to be estimated is selected randomly from the range (0, 2π).

B. PERFORMANCE OF PROPOSED PHASE OFFSET ESTIMATOR

Similar to the previous subsection, this subsection presents the performance of the proposed phase offset estimator. First, its performance is compared with other research works in the literature [21], [22] and [32]. Then its performance is realized for several frequency pulses such as Gaussian, REC, and RC and compared with their respective MCRBs. Finally, the performance of the proposed estimator is observed for AWGN and multipath SUI-3 fading channel.

Fig. 6 shows comparison of variance versus SNR plots of the proposed phase offset estimator for CPM-DSSS system, ML algorithm for CPM system [21], [22] and FFT based phase offset estimator given in [32] applied to CPM system. The value of phase offset is selected randomly for each SNR from range $(0, 2\pi)$. Similar to the previous subsection, it can also observed from the plots that with the increases in SNR, the variance starts decreasing, which leads to improvement in phase offset estimation. Also the proposed phase offset estimator for the CPM-DSSS system has greater than 10 dB better performance than the ML estimator for the CPM system [21], [22] and FFT based phase offset estimator given in [32] applied to CPM system. Therefore, it can be deduced that the proposed estimator for the CPM-DSSS system is performing better than its counter parts.

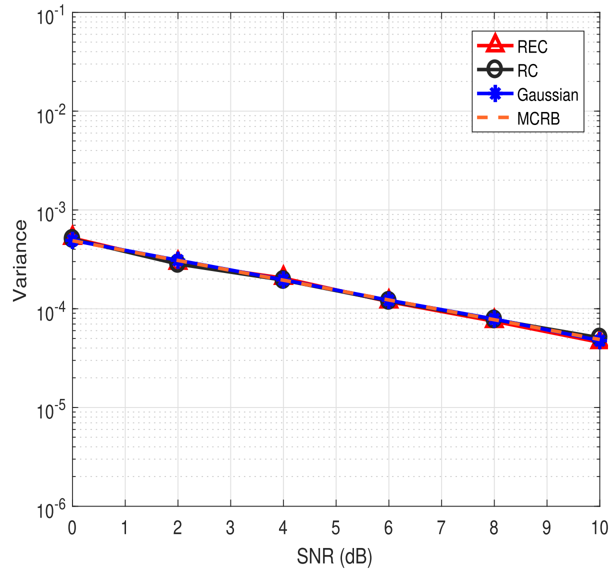

FIGURE 7. Comparison of variance of phase offset estimator versus SNR with MCRB for different *g*(*t*) pulse shapes.

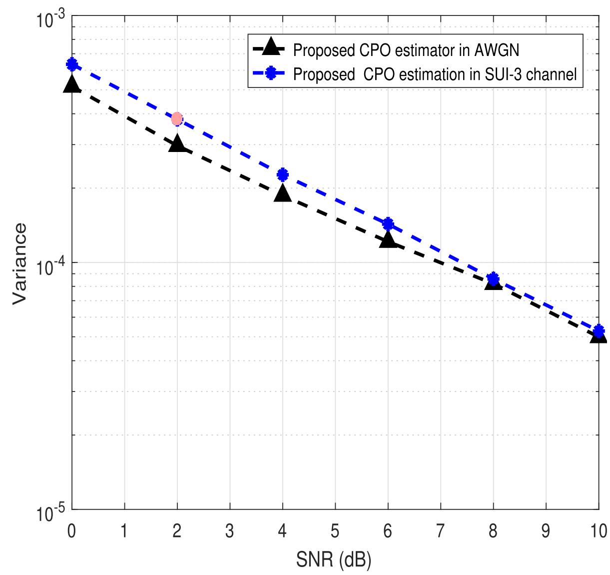

FIGURE 8. Performance of proposed estimator in terms of variance of phase offset estimator versus SNR for AWGN and multipath SUI-3 channel.

Following that, Fig. 7 shows the comparison of proposed phase offset estimator performance to MCRB for phase estimation [35] for three frequency pulses, namely Gaussian, REC, and RC. The fractional delay or timing offset and phase offset are considered to be $0.25T_c$ and $\frac{\pi}{2}$ radians in this case as well. It can be observed that variance of the proposed phase offset estimator approaches the MCRB at all SNRs for all type of frequency pulses considered.

The Fig. 8 indicates the performance of the proposed estimator for the AWGN and SUI-3 multipath fading channel. It is noticed that in comparison to the AWGN channel, the performance degradation for the SUI-3 multipath channel

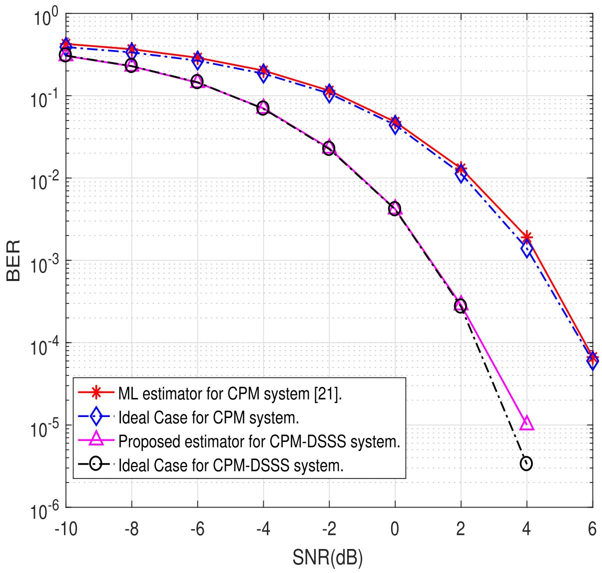

FIGURE 9. Comparison of BER versus SNR plots of the proposed estimator performance for CPM-DSSS system versus ML estimator [21] for CPM systems in AWGN where the parameters used in estimation are taken randomly for each realization.

is almost 1-2 dB at low SNRs, whereas it reaches the performance of AWGN at high SNRs. Hence, the proposed phase offset estimator is robust in multipath channels.

C. BIT ERROR RATE PERFORMANCE

The Fig. 9 shows the system's BER performance comparison of our proposed system with [21]. In both cases, CPM and CPM-DSSS system, the comparison is made with the ideal cases, i.e., when there is no timing and phase offset in the system. The Fig. 9 reflects that the performance of the proposed algorithm coincides with the ideal curve up to the SNR of 2 dB. While ML estimator for the CPM system [21] performance is farther from the ideal curve at almost all SNR as compared to the proposed system. Overall, if two systems are compared, it can be seen that our proposed system performance is approaching more closely to the ideal case at most of the SNR as compared to [21].

V. CONCLUSION

We have presented a novel algorithm to jointly estimate the timing and phase offset for burst mode binary full-response CPM-DSSS system. The performance comparison of the proposed algorithm is done using simulation with other works found in the literature. It is revealed that the proposed estimator outperforms its counterparts. Further, the performance of the joint estimator is compared with MCRB. It is shown that the in case of phase offset estimator its variance coincides with MCRB at all SNRs for all types of frequency pulses considered. Robustness of above algorithm is also tested in SUI-3 multipath fading channel where it is observed that although there is few dB degradation in performance at low SNRs but the performance of SUI-3 channel approaches the AWGN channel performance at high SNRs.

APPENDIX. DERIVATION OF EQUATION

Putting (12) in (10)

$$
\begin{aligned}
Z(\mathbf{d}, \tilde{\tau}) &\approx \sum_{n=0}^{W-1} \int_{nT_c}^{(n+1)T_c} r(t) e^{-j\varphi(t-\tilde{\tau}, \mathbf{d_n})} dt \\
&\approx \sum_{n=0}^{W-1} \int_{nT_c}^{(n+1)T_c} r(t) e^{-j(\phi_n + \pi h d_n \frac{(t-nT_c-\tilde{\tau})}{T_c})} dt \\
&\approx \sum_{n=0}^{W-1} \int_{nT_c}^{(n+1)T_c} r(t) e^{-j\phi_n} e^{-j\left(\pi h d_n (\frac{t-nT_c}{T_c})\right)} e^{j\left(\pi h d_n \frac{\tilde{\tau}}{T_c}\right)} dt \\
&\approx \sum_{n=0}^{W-1} \int_{nT_c}^{(n+1)T_c} r(t) e^{-j\left(\phi_n + \pi h d_n (\frac{t-nT_c}{T_c})\right)} e^{j\left(\pi h d_n \frac{\tilde{\tau}}{T_c}\right)} dt \\
&\approx \sum_{n=0}^{W-1} \int_{nT_c}^{(n+1)T_c} r(t) e^{-j\varphi(t, \mathbf{d_n})} e^{j\left(\pi h d_n \frac{\tilde{\tau}}{T_c}\right)} dt
\end{aligned} \tag{16}
$$

Using (2), we have

$$
Z(\mathbf{d}, \tilde{\tau}) \approx \sum_{n=0}^{W-1} \int_{nT_c}^{(n+1)T_c} r(t) s^*(t) e^{j\left(\pi h d_n \frac{\tilde{\tau}}{T_c}\right)} dt \tag{17}
$$

REFERENCES

[1] A. Celik, J. Tetzner, K. Sinha, and J. Matta, "5G device-to-device communication security and multipath routing solutions," *Appl. Netw. Sci.*, vol. 4, no. 1, pp. 1–24, Dec. 2019.

[2] C. Pöpper, M. Strasser, and S. Čapkun, "Jamming-resistant broadcast communication without shared keys," in *Proc. 18th Conf. USENIX Secur. Symp.* New York, NY, USA: USENIX Association, 2009, pp. 231–248.

[3] S. N. Jenkins, B. A. Kenney, A. J. Majid, H. Moradi, and B. Farhang-Boroujeny, "CP-DSSS: A novel waveform for multiple access in IoT," in *Proc. 2nd 6G Wireless Summit (6G SUMMIT)*, Mar. 2020, pp. 1–5.

[4] A. Bensky, "Wireless local area networks," in *Short-Range Wireless Communication*, A. Bensky, Ed., 3rd ed. London, U.K.: Newnes, 2019, ch. 11, pp. 273–315. [Online]. Available: http://www.sciencedirect.com/science/article/pii/B9780128154052000117

[5] F. Kulsoom, A. Vizziello, H. N. Chaudhry, and P. Savazzi, "Pilot reduction techniques for sparse channel estimation in massive MIMO systems," in *Proc. 14th Annu. Conf. Wireless On-Demand Netw. Syst. Services (WONS)*, Feb. 2018, pp. 111–116.

[6] Y. Liang, J. Ren, and T. Li, "Secure OFDM system design and capacity analysis under disguised jamming," *IEEE Trans. Inf. Forensics Security*, vol. 15, pp. 738–752, 2020.

[7] S. Shehzadi, F. Kulsoom, M. Zeeshan, Q. U. Khan, and S. A. Sheikh, "Joint carrier frequency and phase offset estimation algorithm for CPM-DSSS based secure point-to-point communication," *Turkish J. Elect. Eng. Comput. Sci.*, to be published.

[8] K. Zhou, S. Wang, and E. Zhang, "Coherent RAKE receiver for CPM-based direct sequence spread spectrum," *Math. Problems Eng.*, vol. 2016, Jun. 2016, Art. no. 6971083.

[9] M. Zeeshan, S. A. Khan, and Z. Mehtab, "Data aided algorithm for burst detection in wideband networking waveform with FPGA implementation on SDR platform," in *Proc. 11th Annu. High Capacity Opt. Netw. Emerg./Enabling Technol. (Photon. Energy)*, Dec. 2014, pp. 154–158.

[10] D. K. Asano, T. Hayashi, and R. Kohno, "Modulation and processing gain tradeoffs in DS-CDMA spread spectrum systems," in *Proc. IEEE 5th Int. Symp. Spread Spectr. Techn. Appl.-Spread Technol. Afr.*, vol. 1, Sep. 1998, pp. 9–13.

[11] F. Kulsoom, A. Vizziello, R. Borra, and P. Savazzi, "Reduced complexity Kalman filtering for phase recovery in XPIC systems," *Phys. Commun.*, vol. 29, pp. 112–119, Aug. 2018.

[12] A. Vizziello, P. Savazzi, F. Kulsoom, G. Magenes, and P. Gamba, "A novel galvanic coupling testbed based on PC sound card for intra-body communication links," in *Body Area Networks: Smart IoT and Big Data for Intelligent Health Management*, L. Mucchi, M. Hämäläinen, S. Jayousi, and S. Morosi, Eds. Cham, Switzerland: Springer, 2019, pp. 135–149.

[13] S. Shehzadi, M. Zeeshan, S. A. Sheikh, and Q. U. Khan, "Multimode wideband waveform for software defined radio based on hybrid CPM-CDMA concept," in *Proc. 22nd Int. Multitopic Conf. (INMIC)*, Nov. 2019, pp. 1–4.
[14] O. Omomukuyo, D. Chang, O. A. Dobre, R. Venkatesan, and T. M. N. Ngatched, "Simple sampling clock synchronisation scheme for reduced-guard-interval coherent optical OFDM systems," *Electron. Lett.*, vol. 51, no. 24, pp. 2026–2028, 2015.
[15] A. Masmoudi, F. Bellili, S. Affes, and A. Ghrayeb, "Maximum likelihood time delay estimation from single- and multi-carrier DSSS multipath MIMO transmissions for future 5G networks," *IEEE Trans. Wireless Commun.*, vol. 16, no. 8, pp. 4851–4865, Aug. 2017.
[16] M. Morelli and G. M. Vitetta, "Feedforward joint phase and timing estimation for MSK-type signals," *Eur. Trans. Telecommun.*, vol. 12, no. 4, pp. 327–336, Jul. 2001.
[17] M. Morelli and U. Mengali, "Joint frequency and timing recovery for MSK-type modulation," *IEEE Trans. Commun.*, vol. 47, no. 6, pp. 938–946, Jun. 1999.
[18] J. Huber and W. Liu, "Data-aided synchronization of coherent CPM-receivers," *IEEE Trans. Commun.*, vol. 40, no. 1, pp. 178–189, Jan. 1992.
[19] W. Tang and E. Shwedyk, "ML estimation of symbol timing and carrier phase for CPM in Walsh signal space," *IEEE Trans. Commun.*, vol. 49, no. 6, pp. 969–974, Jun. 2001.
[20] Q. Zhao and G. L. Stuber, "Robust time and phase synchronization for continuous phase modulation," *IEEE Trans. Commun.*, vol. 54, no. 10, pp. 1857–1869, Oct. 2006.
[21] E. Hosseini and E. Perrins, "Maximum likelihood synchronization of burst-mode CPM," in *Proc. IEEE Global Commun. Conf. (GLOBECOM)*, Dec. 2013, pp. 1802–1807.
[22] E. Hosseini and E. Perrins, "Timing, carrier, and frame synchronization of burst-mode CPM," *IEEE Trans. Commun.*, vol. 61, no. 12, pp. 5125–5138, Dec. 2013.
[23] X. Xie and Z. Xu, "Comparison of feedforward synchronization schemes for full-response CPM signals," *IEEE Access*, vol. 5, pp. 27376–27383, 2017.
[24] Z. Xu and Q. Wang, "Autocorrelation function of full-response CPM signals and its application to synchronization," *IEEE Access*, vol. 7, pp. 133781–133786, 2019.
[25] Q. Lin, S. Mohan, and M. A. Weitnauer, "Interference-insensitive synchronization scheme of MSK for transmit-only wireless sensor network," in *Proc. IEEE Int. Conf. Commun. (ICC)*, May 2016, pp. 1–6.
[26] M. Golay, "Complementary series," *IRE Trans. Inf. Theory*, vol. 7, no. 2, pp. 82–87, Apr. 1961.
[27] S. S. B. S. Abdullah, O. O. Khalifa, F. A. Rahman, and H. Nasir, "Performance evaluation on error probabilities of coded BPSK system using the linear (23, 12) Golay code with hard-decision decoding," in *Proc. IEEE Int. Conf. Smart Instrum., Meas. Appl. (ICSIMA)*, Aug. 2019, pp. 1–4.
[28] D. K. Asano, T. Hayashi, and R. Kohno, "Modulation and processing gain tradeoffs in DS-CDMA spread spectrum systems," in *Proc. IEEE 5th Int. Symp. Spread Spectr. Techn. Appl.-Spread Technol. Afr.*, vol. 1, Sep. 1998, pp. 9–13.
[29] T. Aulin and C. Sundberg, "Continuous phase modulation–Part I: Full response signaling," *IEEE Trans. Commun.*, vol. 29, no. 3, pp. 196–209, Mar. 1981.
[30] T. Aulin, N. Rydbeck, and C.-E. Sundberg, "Continuous phase modulation–Part II: Partial response signaling," *IEEE Trans. Commun.*, vol. 29, no. 3, pp. 210–225, Mar. 1981.
[31] W. Tang and E. Shwedyk, "ML estimation of symbol timing and carrier phase for CPM in Walsh signal space," *IEEE Trans. Commun.*, vol. 49, no. 6, pp. 969–974, Jun. 2001.
[32] P. Jg, *Digital Communications*. New York, NY, USA: McGraw-Hill, 2001.
[33] P. Singh, H. B. Mishra, A. K. Jagannatham, and K. Vasudevan, "Semi-blind, training, and data-aided channel estimation schemes for MIMO-FBMC-OQAM systems," *IEEE Trans. Signal Process.*, vol. 67, no. 18, pp. 4668–4682, Sep. 2019.
[34] M. Zeeshan and S. Khan, "Robust sampling clock recovery algorithm for wideband networking waveform of SDR," *Int. J. Commun. Netw. Inf. Secur.*, vol. 5, no. 1, p. 10, Apr. 2013.
[35] U. Mengali, *Synchronization Techniques for Digital Receivers*. New York, NY, USA: Springer, 2013.
[36] V. Erceg, K. Hari, M. Smith, D. Baum, K. Sheikh, C. Tappenden, J. Costa, C. Bushue, A. Sarajedini, R. Schwartz, and D. Branlund, "Channel models for fixed wireless applications," IEEE 802.16 Broadband Wireless Access Working Group, IEEE, Piscataway, NJ, USA, Tech. Rep. 802.16.3c-01/29r4, Jan. 2001. [Online]. Available: https://www.researchgate.net/publication/243777280_Channel_Models_for_Fixed_Wireless_Application

SAIMA SHEHZADI received the B.Sc. degree (Hons.) in software engineering and the master's degree in telecommunication engineering from the University of Engineering and Technology, Taxila, Pakistan, in 2006 and 2011, respectively. She is currently pursuing the Ph.D. degree with the NUST College of Electrical and Mechanical Engineering. She served as an Assistant Professor at Hamdard University—Islamabad Campus, from 2012 to 2015. Her current research interest includes synchronization in 5G point-to-point communication systems.

SHAHZAD AMIN SHEIKH received the B.S. degree in electrical engineering from the Eastern Mediterranean University (EMU), Famagusta, Northern Cyprus, in 1995, the master's degree in electrical engineering from the University of New South Wales (UNSW), Sydney, NSW, Australia, in 2002, and the Ph.D. degree in electrical engineering from Southwest Jiaotong University, Chengdu, China, in 2008. He is currently a Professor with the Department of Electrical Engineering, College of Electrical and Mechanical Engineering, National University of Science and Technology (NUST), Islamabad, Pakistan. His current research interests include signal processing and its applications in digital communication.

FARZANA KULSOOM received the B.Sc. degree in computer engineering and the master's degree in telecommunication engineering from the University of Engineering and Technology, Taxila, Pakistan, in 2006 and 2012, respectively, and the Ph.D. degree in wireless communication and signal processing from the University of Pavia, Italy, in 2019. She is currently working as an Assistant Professor at the University of Engineering and Technology. Her current research interests include signal processing, next-generation communication systems, machine learning applied to signal processing, and MIMO-based communication.

MUHAMMAD ZEESHAN received the Ph.D. degree in electrical engineering, with a focus on wireless communications, from the National University of Sciences and Technology (NUST), Pakistan, in 2015. Since July 2010, he has been with the Center for Advanced Research in Engineering (CARE), Pakistan, first as a Senior Design Engineer and then as a Member Technical Staff, since July 2014. In March 2016, he joined the Faculty of the College of Electrical and Mechanical Engineering, NUST, where he is currently an Assistant Professor of wireless communications with the Department of Electrical Engineering.

QASIM UMAR KHAN received the B.E. and M.S. degrees in computer and electrical engineering, and the Ph.D. degree in electrical engineering from the College of Electrical and Mechanical Engineering, National University of Sciences and Technology, Islamabad, Pakistan, in 2009, 2011, and 2016, respectively. He is currently an Assistant Professor with the Department of Electrical Engineering, NUST. He has various reputable journals and conference publications to his name. He is currently working towards the designs of MIMO antennas for 5G/6G applications. His research interests include planar antenna designs, theory of characteristic modes, microwave devices, digital communication, and digital signal processing.